Supplementary Material

Biomimetic porous cellular foam with space thermal domain for efficient uranium extraction from seawater

Yachao Xu,[a, b] Jiahui Zhu,[a, b*] Hongsen Zhang,[a, b] Qi Liu,[a, b, c] Jingyuan Liu,[a, b] Rongrong Chen,[a, b] Jing Yu,[a, b] Jun Wang[a, b*]

a. Key Laboratory of Superlight Materials and Surface Technology, Ministry of Education, Harbin Engineering University, Harbin 150001, China

b. College of Materials Science and Chemical Engineering, Harbin Engineering University, Harbin 150001, China

c. Hainan Harbin Institute of Technology Innovation Research Institute Co., Ltd. Hainan 572427, China

Corresponding author: Jiahui Zhu

E-mail address: jiahuizhu@hrbeu.edu.cn

Corresponding author: Jun Wang

E-mail address: zhqw1888@sohu.com

Characterizations

Powder X-ray diffraction (XRD) patterns were analyzed by a BrukerD8 Advance diffractometer with monochromatized Cu Kα radiation (λ = 1.5406 Å, generated at an acceleration voltage of 40 kV and an applied current of 20 mA). The refined structure and morphology of the samples were recorded by scanning electron microscopy (SEM, FEISirion 200 instrument operated at 15 kV) and transmission electron microscopy (TEM, Tecnai G2 F20) at an acceleration voltage of 200 kV. The X-ray photoelectron spectroscopy (XPS) measurements were performed to investigate the surface states using a ULTRAAXIS DLD with an Al Kα (1253.6 eV) achromatic X-ray source by referencing to the C1 s peak at 284.6 eV. Diffuse reflectance spectroscopy (DRS) was carried out on a UV–vis spectrophotometer (Lambda 950 (PerkinElmer, USA)) in the range of 200-1800 nm, with fine $BaSO_4$ powder as a reference. Nitrogen adsorption-desorption isotherms at 77 K were collected on an AUTOSORB-1 (Quantachrome Instruments) nitrogen adsorption apparatus. The Brunauer-Emmett-Teller (BET) equation was used to estimate the specific surface area. Pore size distributions were measured using the Barrett-Joyner-Halenda (BJH) method from the adsorption branch of the isotherms. The pl spectrum of the sample was detected on a PE LS 55spectrophotometer with an excitation wavelength of 325 nm.

Photocatalytic activity measurements

In a typical photocatalytic experiment, 20 mg of CPAO/PDA, 20 ml of methanol, and 80 mL of 100 ppm UO_2^{2+} stock solution were added to a 100 mL single-neck

flask. Then the suspension was transferred into a reactor and the pH value was adjusted with 0.1 M NaOH and HCl solution. Before irradiation, the reactor was bubbled with N_2 in the dark for 120 minutes to remove oxygen to ensure anaerobic conditions and achieve adsorption-desorption equilibrium. Subsequently, a 300W high-pressure xenon lamp was used as the light source. During the reaction process, a certain volume of solution was extracted at a specific time and analyzed with ICP-ms to detect the concentration of UO_2^2.

Calculation details

MD simulations were performed on three polymer MF-CPAO/CN models: the neutral, anion and cation types. Polymer amorphous models were constructed with five polymer chains per simulation box. The initial simulation model was put into a cubic box (8.0 nm per side) with an initial density of about 0.0510 g cm^{-3}, and then the equilibration simulation was achieved by the five cycles anneal. Finally, the polymer CPAO/CN obtained was solvated in the solution box including 5,000 water molecules and 8 uranyl ions. Na^+ or Cl^- ions were added to make the solution neutral during the simulations. In this work, the uranyl concentration was set at 0.09 mol l^{-1} to reduce the simulation cost. The initial models were built using the Packmol package.

A consistent valence forcefield (cvff) was then used with the Large-scale Atomic/Molecular Massively Parallel Simulator (LMMPS) package in all the MD simulations. The polymer chain topology file was done with the aid of Materials Studio software. The SPC water model was used. The partial charges for the neutral,

anion and cation types of CPAO/CN monomers used the restrained electrostatic potential charges, which were obtained using the quantum mechanism calculation in the solvation model at the b3lyp/6-31g* level of theory using Gaussian 09 and fitted by the electronic wavefunction analysis program using Multiwfn. The detailed simulation steps were as follows: (1) the initial model was energy-minimized to remove the system strain; (2) 200 ps NVT dynamics simulations were carried out, and the initial velocities were generated on the basis of a Maxwellian distribution at 300 K; (3) 2 ns equilibrium NPT dynamics simulations were carried out; and (4) the independent sampling analyses of 10 ns NPT MD simulations for each case were performed. A time step of 2.0 fs was used in all the simulations. The temperature was controlled using a velocity-rescaling thermostat with a relaxation time of 0.1 ps. The Berendsen pressure scaling was performed isotropically by coupling to a pressure bath of 10^5 Pa (with a time constant of 1.0 ps). The particle mesh Ewald summation method was used to calculate the electrostatic potential under periodic boundary conditions in all three spatial dimensions.

Solar-driven water evaporation experiments

The solar-driven water evaporation rate and the solar thermal conversion efficiency were evaluated by the following experiments. All solar-driven water evaporation experiments were conducted by using a solar simulator (CEL-PE300L) with an AM 1.5 filter. A homemade vessel with a surface area of 7.1 cm^2 was used as the evaporation device. A certain amount of 3.5 wt% NaCl solution was added into the

vessel. Then, CPAO/PDA was added into the vessel on the saline water surface. Afterwards, the whole vessel was placed on an analytical electronic balance connected with a computer and illuminated by a light source as mentioned above. An infrared camera was used to measure the surface temperature of CPAO/PDA. For the cyclic evaporation tests, the test time of each cycle was 1 h, CPAO/PDA-2 was washed with water and vacuum dried after each test, and then used for the next cycle of evaporation. The solar energy efficiency (η) for the solar water evaporation can be calculated according to the following equation:

$$\eta = mh_{LV}/C_{opt}P_0 \quad (1)$$

where m is the steady-state water evaporation rate (kg m^{-2} h^{-1}), hLV is the latent enthalpy of vaporization (kJ kg-1) of the liquid-vapor phase change, Copt is the optical concentration and P0 is the solar optical power of one sun (1 kW m^{-2}). The value of hLV varies with temperature. In our experiments, due to the narrow temperature range and the evaporation through large inter-particle voids, the value of hLV only varies very slightly with temperature and thus a constant value of 2260 kJ kg^{-1} is adopted for the calculation.

Adsorption performance in U(VI) aqueous solution

Firstly, the 1000 mg L^{-1} U-containing aqueous solution was prepared through 4.22 g of $UO_2(NO_3)_2$ diluting to 2.00 L with 0.5 mL of 1.0 M HNO_3. Secondly, the specific concentration of U-containing aqueous solution was prepared by diluting above solution. Subsequently, the concentration of U(VI) before and after adsorbing was

measured by ICP. Finally, the adsorption capacity of U(VI) was calculated according to Equation (S1) [1]:

$$q_e = \frac{V}{m} \times (C_0 - C_e) \quad \text{(S1)}$$

wherein, q_e is the adsorption capacity of adsorbents, V is the volume of U-containing aqueous solution, m is the mass of the adsorbents, C_0 is the initial concentration, and C_e is the concentration after adsorption.

The effect of pH on adsorption performance:

Primarily, the concentration of U-containing solution was enacted to 100 mg L^{-1}, and the pH was adjusted by 1.0 M NaOH/HNO_3 to 3.0, 4.0, 5.0, 6.0, 7.0, 8.0, and 9.0, respectively. Secondary, 20 mg adsorbents and 50 mL 100 mg L^{-1} U-containing solution were mixed to a 200 mL conical flask in water bath oscillator for 8 h at 298 K. Similarly, the adsorption capacity of U(VI) was also calculated according to Equation (S1).

The effect of contact time on adsorption performance:

The concentration and pH of U-containing solution was set to 100 mg L^{-1} and 6.0, respectively. Similarly, 20 mg adsorbents and 50 mL 100 mg L^{-1} U-containing solution were mixed to a 200 mL conical flask in water bath oscillator at 298 K, and the adsorption capacity of U(VI) was also calculated according to Equation (S1). However, in order to study the reaction kinetics in the adsorption process, the contact

time was set to 10, 20, 30, 60, 120, 180, 300, 720, 1020, and 1440 min, respectively. Furthermore, the data of adsorption was fitted with the pseudo-first-order, pseudo-second-order, and intra-particle diffusion models according to the Equation (S2), Equation (S3), and Equation (S4), respectively[1]:

$$\ln\left(q_e - q_t\right) = \ln q_e - k_1 t \quad \text{(S2)}$$

$$\frac{t}{q_t} = \frac{1}{k_2 q_t} + \frac{t}{q_e} \quad \text{(S3)}$$

$$q_e = k_{ip}\sqrt{t} + C \quad \text{(S4)}$$

wherein, q_e and q_t is the adsorption capacity at the contact and equilibrium time, respectively, k_1 and k_2 are the rate constant, k_{ip} is internal diffusion constant.

The effect of temperature and initial concentration on adsorption performance:

Similarly, the pH of U-containing solution was set to 6.0, and 20 mg adsorbents and 50 mL U-containing solution were mixed to a 200 mL conical flask in water bath oscillator for 8 h, and the adsorption capacity of U(VI) was also calculated according to Equation (S1). However, the initial concentration was enacted to 5.38, 15.86, 43.58, 120.50, 187.00, 256.50, and 286.90 mg L^{-1}, respectively, and the temperature was set to 298 K, 308 K, and 318 K, respectively. In order to evaluate the material's adsorption isotherm, the data of adsorption was fitted to the Langmuire, Freundlich, and Dubinin-Radushkevich isotherm models according to Equation (S5), Equation (S6), and Equation (S7-8), respectively[1]:

$$\frac{C_e}{q_e} = \frac{C_e}{q_m} + \frac{1}{k_1 q_m} \quad \text{(S5)}$$

$$\log q_e = \log k + \frac{1}{n}\log C_e \quad \text{(S6)}$$

$$\ln q_e = \ln q_m - \beta\varepsilon^2 \quad (S7)$$

$$\varepsilon = RT\ln\left(1 + \frac{1}{C_e}\right) \quad \text{(S8)}$$

wherein, q_e is the adsorption capacity at equilibrium, q_m is the maximum adsorption capacity, C_e is the equilibrium concentration, the k_1 and k_2 is an equilibrium constant and approximate indicator of adsorption capacity, respectively, $\frac{1}{n}$ is a function of the adsorption strength, and β is the activity coefficient.

The effect of adsorption-desorption cycle on adsorption performance:

Similarly, the concentration and pH of U-containing solution was set to 100 mg L^{-1} and 6.0, respectively, and 20 mg adsorbents and 50 mL 100 mg L^{-1} U-containing solution were mixed to a 200 mL conical flask in water bath oscillator at 298 K, and the adsorption capacity of U(VI) was also calculated according to Equation (S1). Subsequently, the 0.1 M HNO_3 was used as desorbent to implement 5 cycles test.

The effect of V(V) concentration on adsorption performance:

Similarly, the pH of solution was set to 6.0, and 10 mg adsorbents and 100 mL solution were mixed to a 200 mL conical flask in water bath oscillator at 298 K, and

the adsorption capacity was also calculated according to Equation (S1). However, when the concentration of U(VI) was set to 100 mg L^{-1}, the concentration of V(V) was set to 5, 25, 30, 60, and 125 mg L^{-1}, respectively; when the concentration of U(VI) was set to 8 mg L^{-1}, the concentration of V(V) was set to 0.5, 1.0, 2.0, 4.0, and 8.0 mg L^{-1}, respectively; when the concentration of U(VI) was set to 100 μg L^{-1}, the concentration of V(V) was set to 10, 20, 50, 100, and 120 μg L^{-1}, respectively; when the concentration of U(VI) was set to 20 μg L^{-1}, the concentration of V(V) was set to 5.0, 10, 20, 30, and 40 μg L^{-1}, respectively.

Adsorption performance in simulated seawater:

The different concentrations of U-containing aqueous solution were prepared by dilution method. In addition, 33.35 g sea salt was added to 1.0 L above solution to prepare the simulated seawater solutions, including 3, 10, 50, 100, 300, and 500 μg L^{-1}. Similarly, 10 mg adsorbents and 50 mL solution were mixed to a 200 mL conical flask in water bath oscillator for 8 h at 298 K, and the adsorption capacity was also calculated according to Equation (S1).

Anti-bacterial activity experiment

Staphylococcus aureus (*S.aureus:* Gram-positive bacteria) in this experiment was cultured on liquid Luria broth (LB) medium [1.0 L ultrapure water, 10.0 g tryptone, 5.0 g yeast extract, and 10.0 g NaCl]. The adsorbents and the commodities were sterilized. The prepared liquid LB was divided into 250 mL glass bottles, and sealed. After sterilization, inoculate in an ultra-clean bench, and used the corresponding strain

after low-temperature thawing, and then placed it in an incubator at 37 °C for 24 h. Subsequently, a bacterial suspension was prepared (the certain amounts of bacteria into a sterilized liquid medium), and then placed in shaker at 30 °C and 150 rpm for 24 h. After centrifuging the cultured bacterial suspension, it was suspended in a phosphate buffer with an isotonic solution pH=7.4, and the concentration of the controlled bacteria was roughly on the order of 10^6 CFU/mL. Finally, the dropper draws 10 mL of LB medium to rinse the surface of the adsorbents, then the 10 μL of rinsing solution was diluted to 10 mL, and then 10 μL of the diluted solution was taken on the solid medium, and used a sterilized flat plate. The bacterial solution was evenly spread on the culture medium, and the culture medium was placed in the incubator at 37 °C for 24 h[2].

Actual seawater adsorption experiments

The adsorbents were placed in the actual seawater, and after floating for 30 days, it was completely retrieved for desorption experiment. Subsequently, the 0.1 M HNO_3 was used as desorbent to obtain the U-containing solution. Finally, the above solution was diluted to 100 times for ICP testing.

Supplementary Figures and Tables

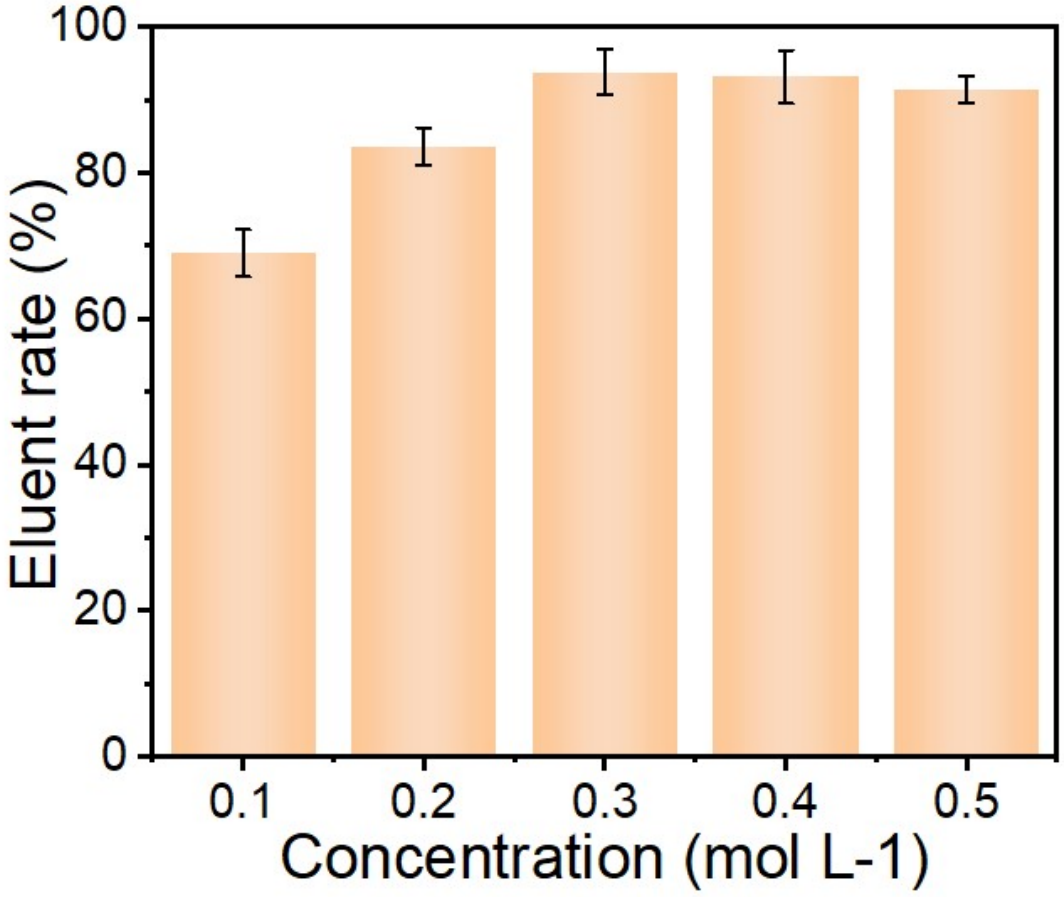

Figure S1. Desorption efficiency of different concentrations of HNO3 on CPAO/CN.

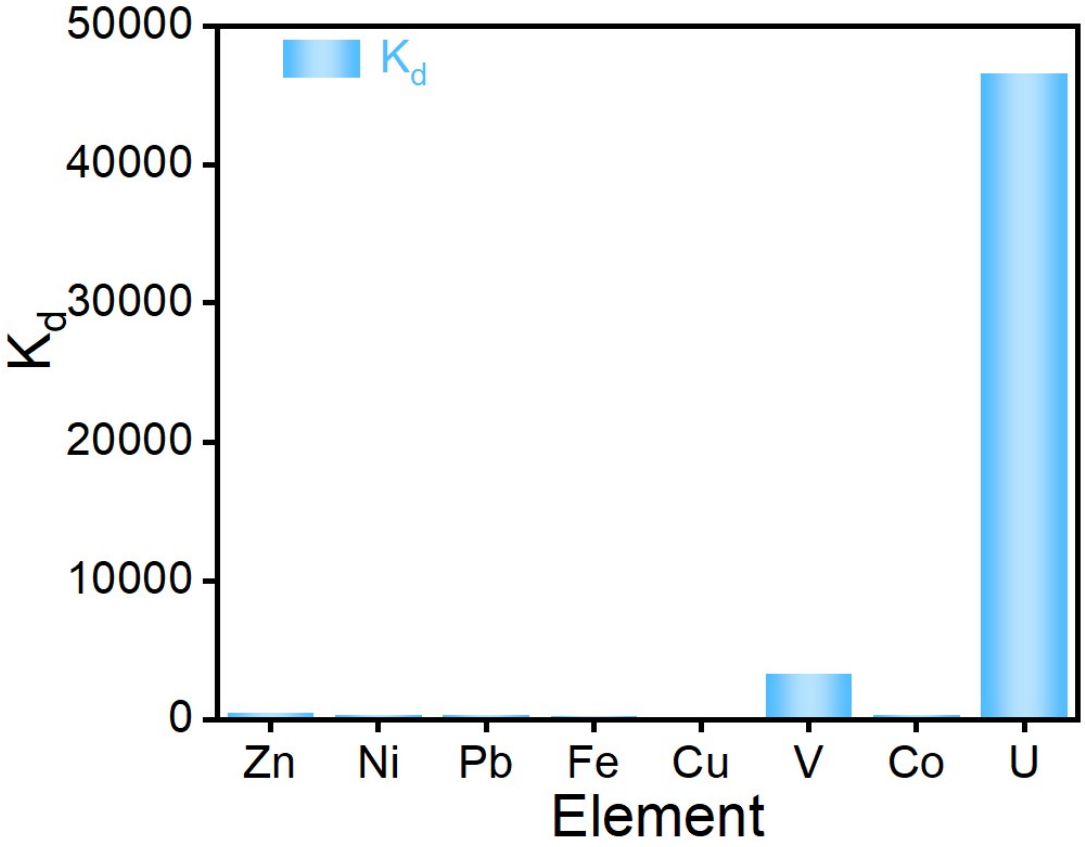

Figure S2. Ion Distribution Coefficient of CPAO/CN.

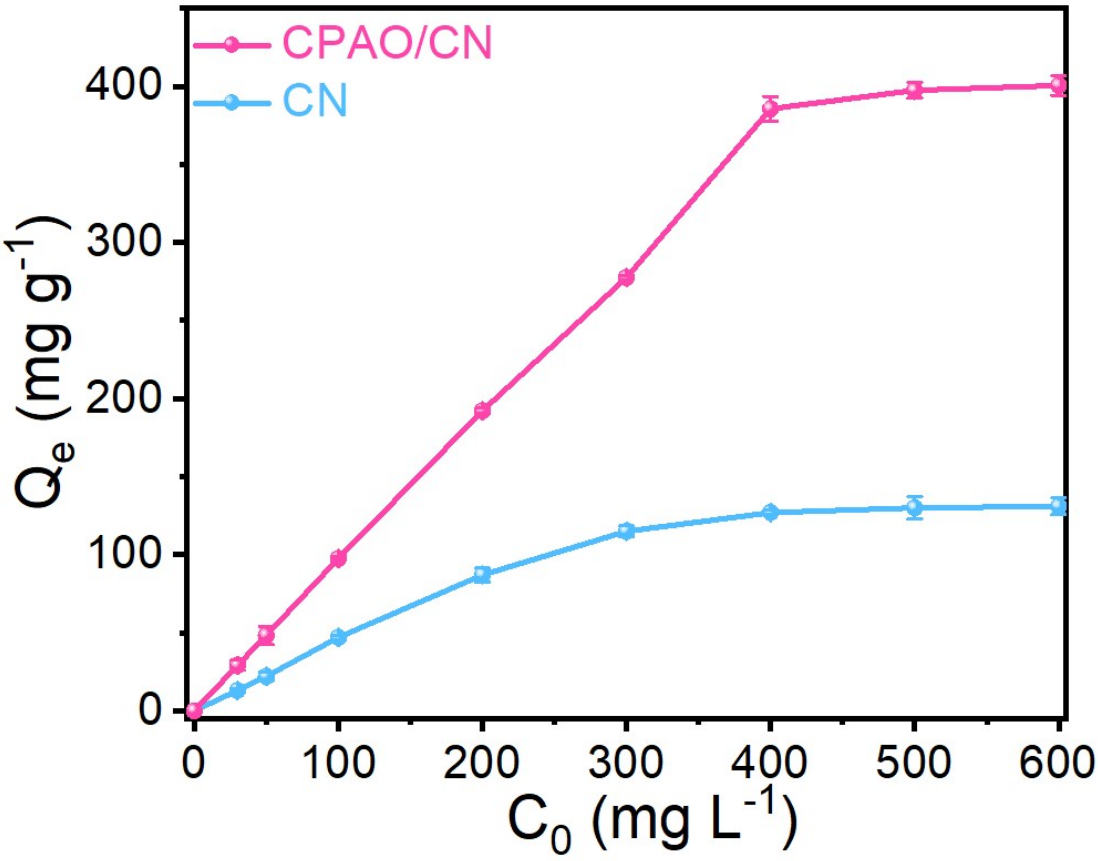

Figure S3. Effects of eifferent initial uranium solution concentrations on the adsorption capacity of CPAO/CN and CN.

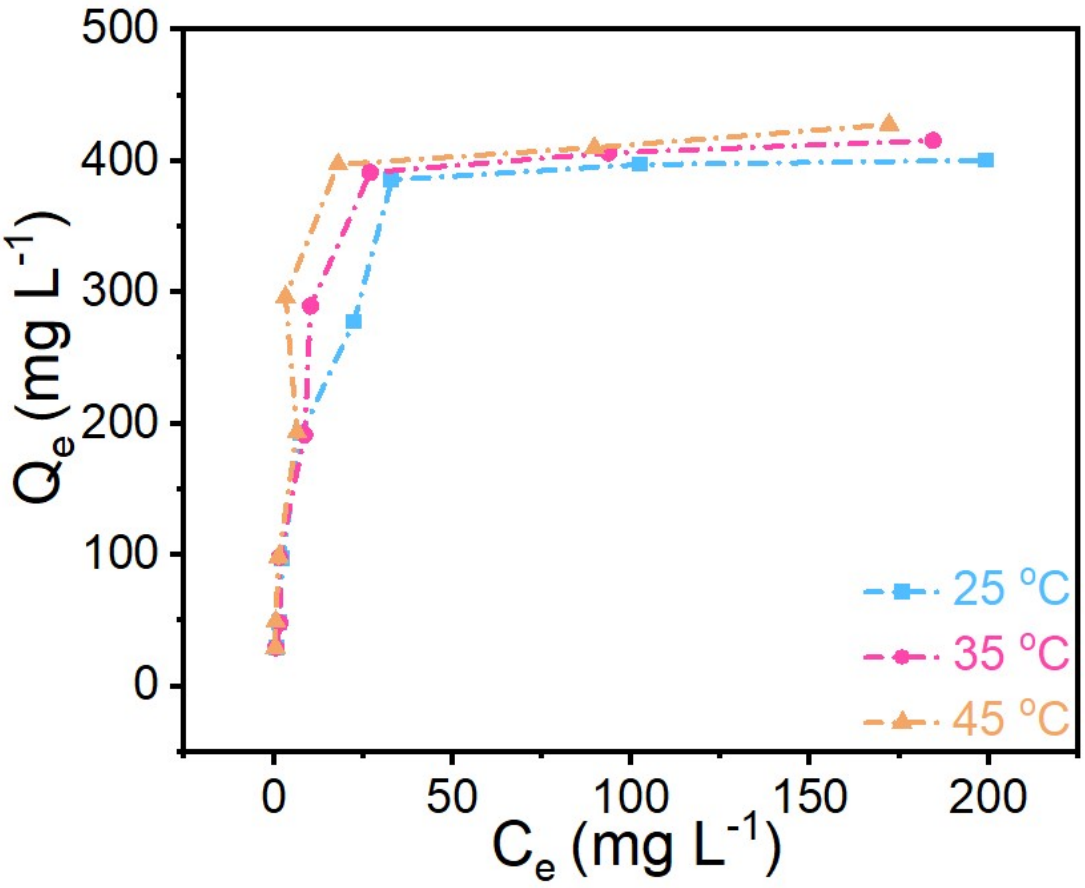

Figure S4. Effects of U(VI) initial concentration on the adsorption performance of CPAO/CN at different temperatures.

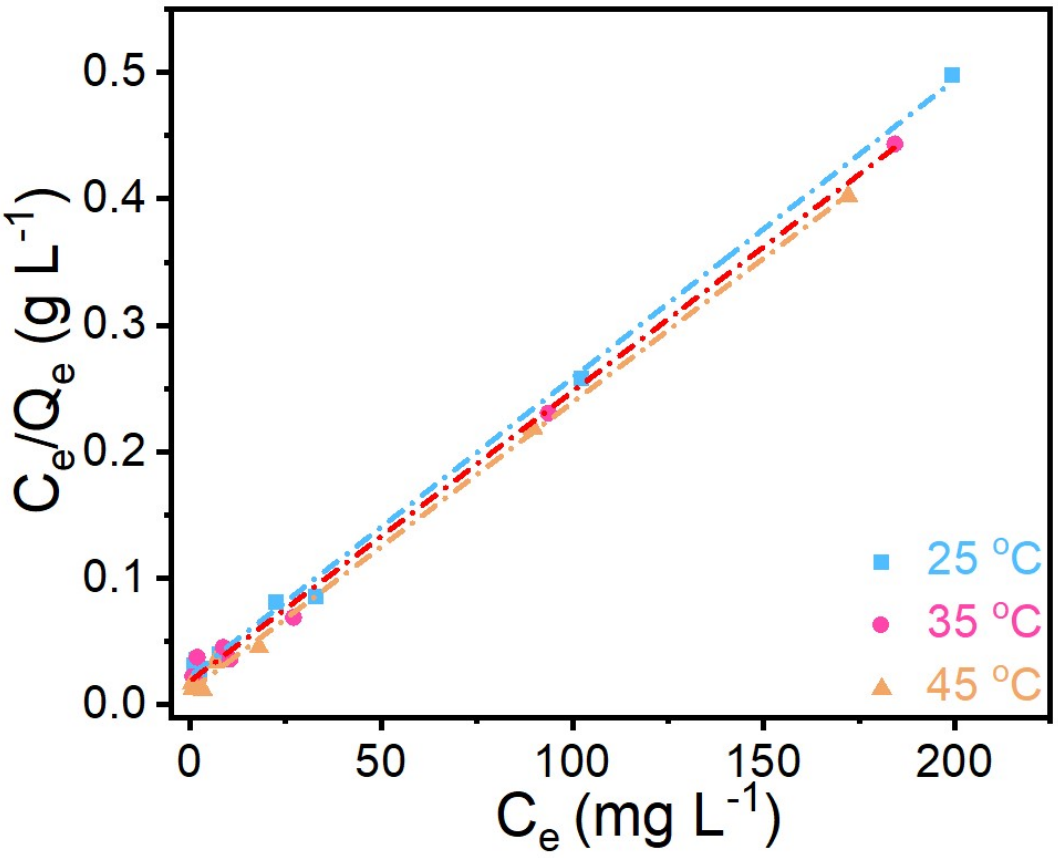

Figure S5. Langmuir model of CPAO/CN.

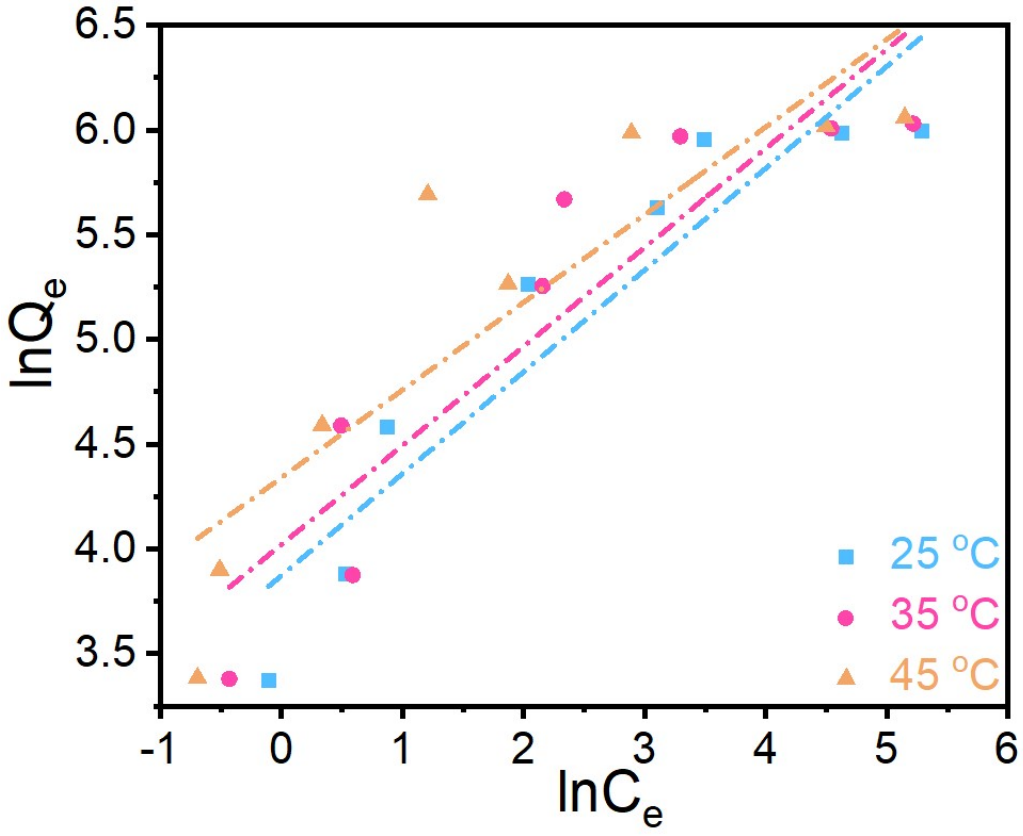

Figure S6. Freundlich model of CPAO/CN.

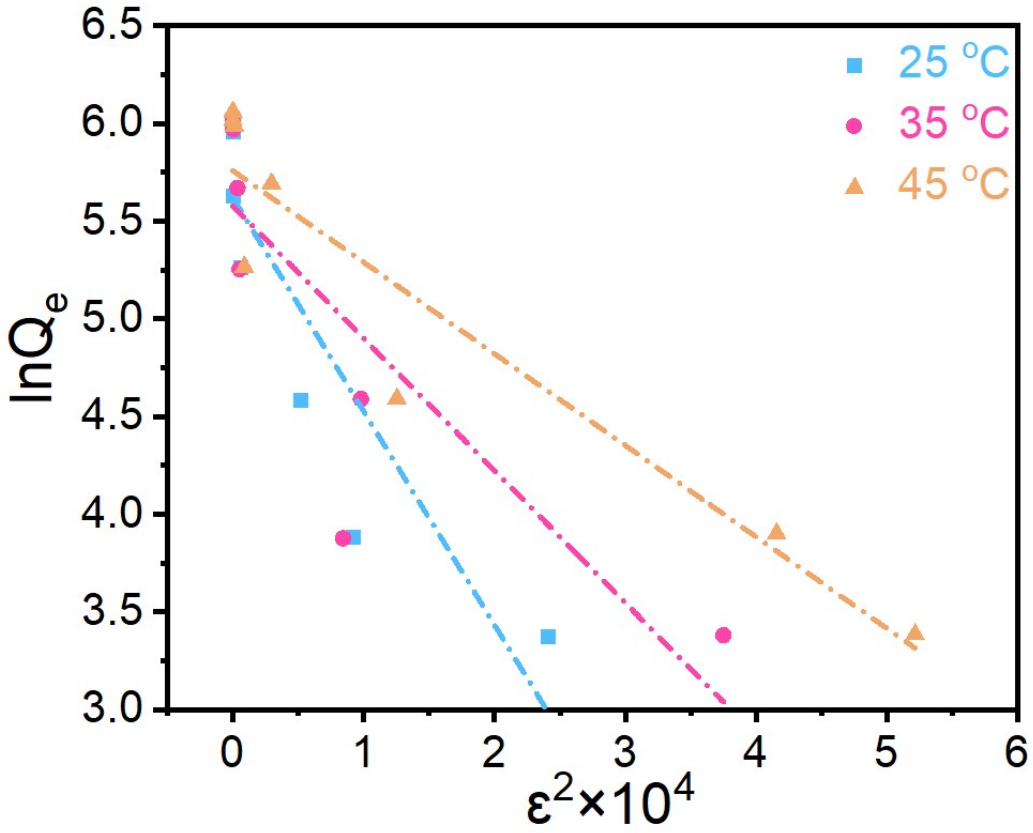

Figure S7. Dubinin-Radushkevich model of CPAO/CN.

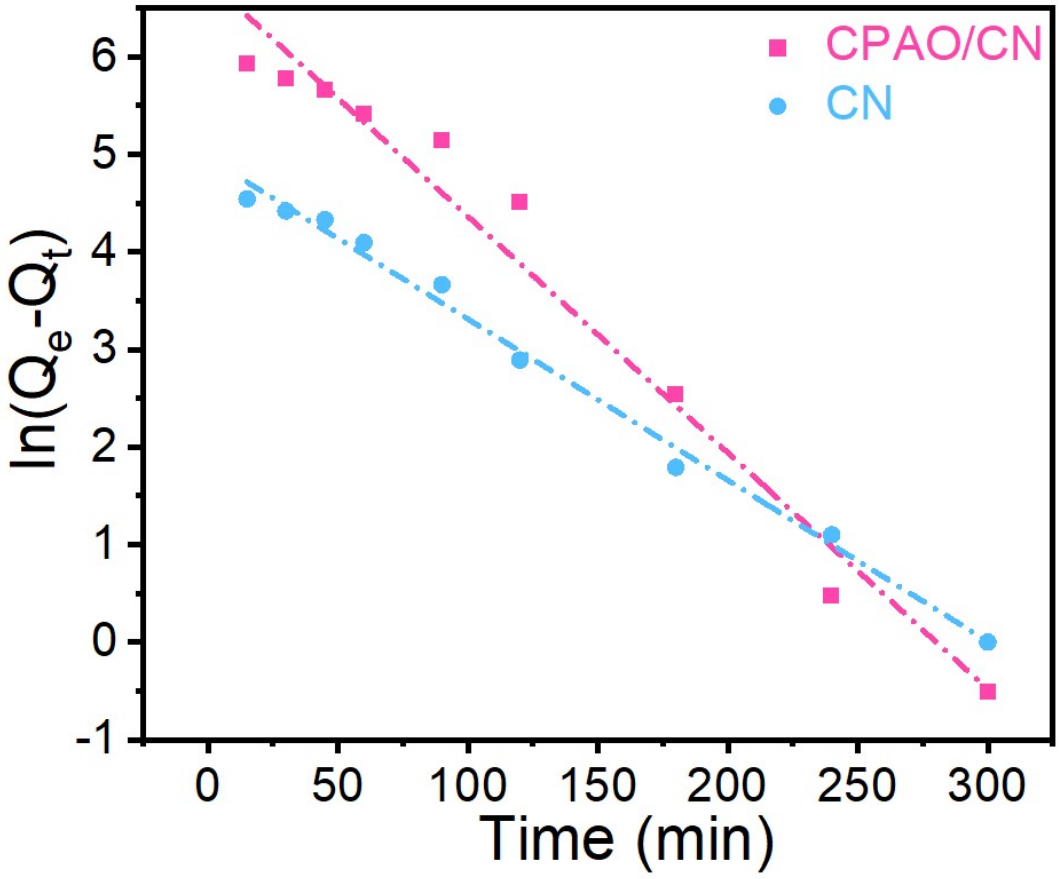

Figure S8. Pseudo-first-order kinetic fit of CPAO/CN and CN.

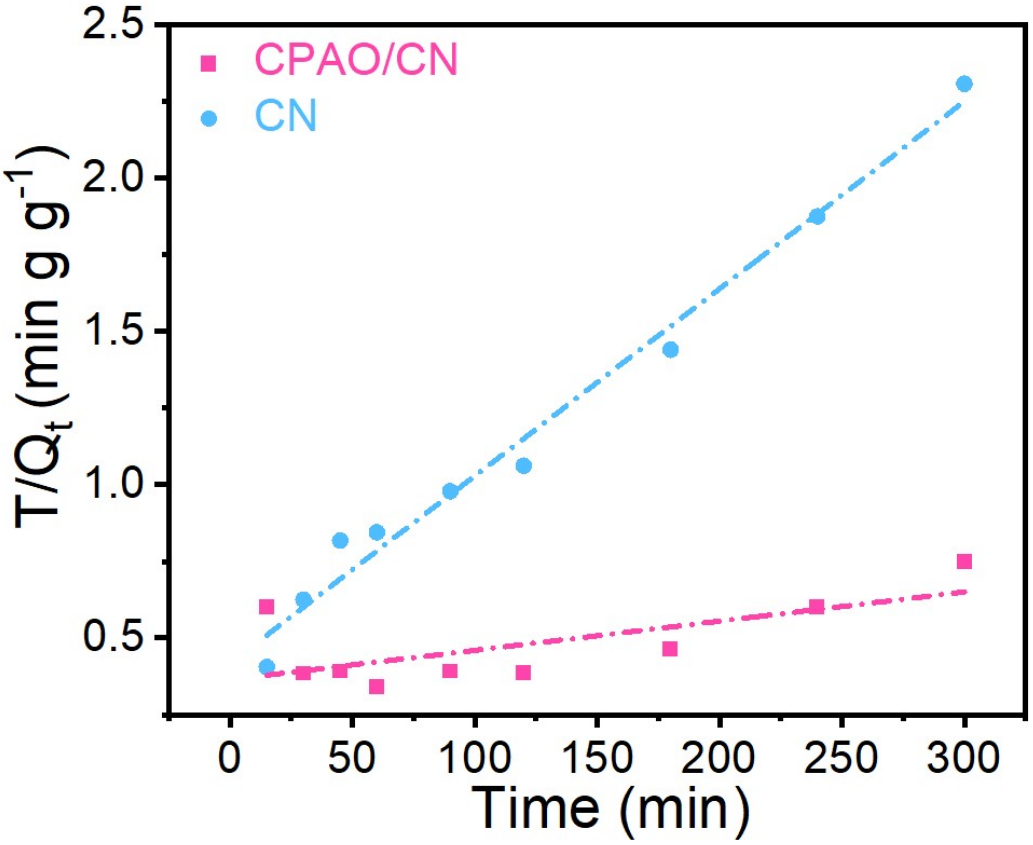

Figure S9. Pseudo-second-order kinetic fit of CPAO/CN and CN.

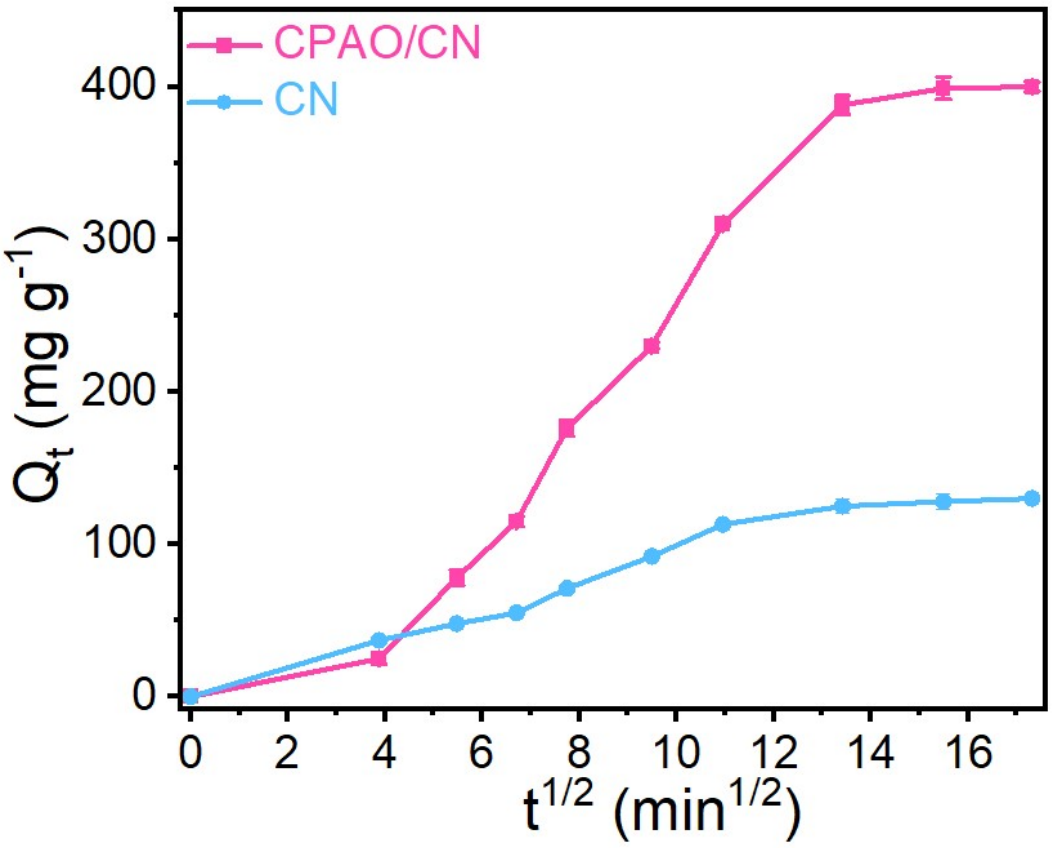

Figure S10. W-M kinetic model of CPAO/CN and CN.

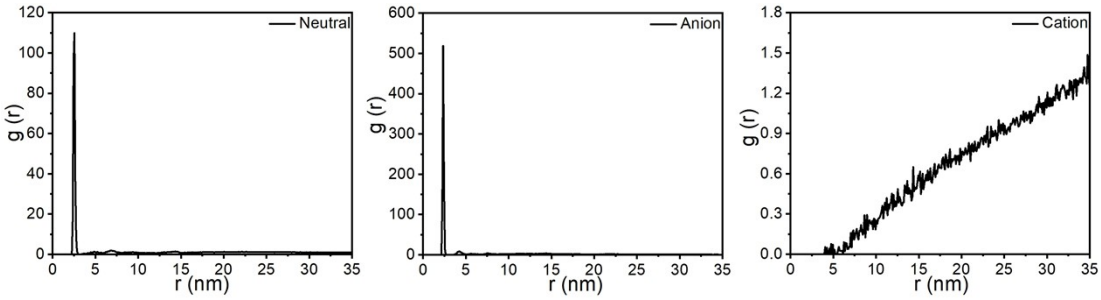

Figure S11. O-U radial distribution functions of three CPAO/CN models.